

# Stress-induced Condensation of Bacterial Genomes Results in Re-pairing of Sister Chromosomes

## IMPLICATIONS FOR DOUBLE STRAND DNA BREAK REPAIR\*<sup>§</sup>

Received for publication, March 28, 2013, and in revised form, July 22, 2013. Published, JBC Papers in Press, July 24, 2013, DOI 10.1074/jbc.M113.473025

Nelia Shechter<sup>†</sup>, Liron Zaltzman<sup>†</sup>, Allon Weiner<sup>†</sup>, Vlad Brumfeld<sup>§</sup>, Eyal Shimoni<sup>§</sup>, Yael Fridmann-Sirkis<sup>†</sup>, and Abraham Minsky<sup>†1</sup>

From the Departments of <sup>†</sup>Structural Biology and <sup>§</sup>Chemical Research Support, The Weizmann Institute of Science, Rehovot 76100, Israel

**Background:** Genome-wide homology search is inconsistent with the emerging view of bacterial genome morphology.

**Results:** Stress-induced genome condensation proceeds through nonrandom convergence of sister chromosomes that culminates in spatial proximity of homologous sites.

**Conclusion:** Chromosome convergence enables repair of double strand DNA breaks.

**Significance:** Exposure to diverse stressful conditions primes bacteria to cope with detrimental DNA lesions.

Genome condensation is increasingly recognized as a generic stress response in bacteria. To better understand the physiological implications of this response, we used fluorescent markers to locate specific sites on *Escherichia coli* chromosomes following exposure to cytotoxic stress. We find that stress-induced condensation proceeds through a nonrandom, zipper-like convergence of sister chromosomes, which is proposed to rely on the recently demonstrated intrinsic ability of identical double-stranded DNA molecules to specifically identify each other. We further show that this convergence culminates in spatial proximity of homologous sites throughout chromosome arms. We suggest that the resulting apposition of homologous sites can explain how repair of double strand DNA breaks might occur in a mechanism that is independent of the widely accepted yet physiologically improbable genome-wide search for homologous templates. We claim that by inducing genome condensation and orderly convergence of sister chromosomes, diverse stress conditions prime bacteria to effectively cope with severe DNA lesions such as double strand DNA breaks.

A particularly deleterious type of DNA damage is double strand DNA breaks (DSBs)<sup>2</sup> (1). An important repair mechanism of this lesion proceeds through homologous repair, which relies on the interaction of chromosomal ends generated by DSBs with homologous sequences that act as templates (2, 3). Accordingly, homologous repair strictly depends on the accessibility of such templates to severed DNA ends. In eukaryotes, this prerequisite is met by cohesin-mediated apposition of sister chromatids (4–6). In contrast, segregation of bacterial sister

chromosomes shortly following replication (7–14) prevents on-site access of DSBs to their repair templates. It is thus generally assumed that for homologous repair to occur in bacteria, severed DNA ends need to conduct a genome-wide homology search (2, 3).

Genome-wide search is, however, inconsistent with the emerging view of genome morphology in bacteria. Specifically, recent studies demonstrated that chromosomal sites in bacteria are persistently localized at specific cytoplasmic addresses (9, 15–20) and that bacterial genomes consist of multiple domains that are spatially confined and mutually inaccessible (21, 22). Such a genome organization, which indicates a highly constrained motion of chromosomal sites, implies that a genome-wide search is unlikely. This claim is supported by the finding that diffusion of genomic sites is substantially slower than that revealed by proteins (23), indicating that homology search conducted by chromosomal sites for homologous templates cannot be considered in terms of a search performed by proteins for their cognate DNA sequences (24). Indeed, although significant insights into the process by which DSBs *identify* their homologous repair templates have recently been achieved (25, 26), the question how such lesions *find* these templates, which are embedded within a genomic-length DNA, remains unanswered (24).

It is becoming increasingly evident that exposure of bacteria to diverse detrimental conditions results in massive genome condensation (27–32). The physiological implications of this apparently generic stress response, which was recently demonstrated to occur also in archaea (33), remain unclear. By using fluorescent markers to locate specific *Escherichia coli* chromosomal sites, we show that stress-induced genome condensation proceeds through an orderly convergence of segregated sister chromosomes rather than through random DNA collapse. This convergence is suggested to initiate at the replication forks and to be mediated by the recently demonstrated ability of identical double-stranded DNA molecules to specifically identify each other and generate robust complexes (34, 35). We propose that the ensuing proximity of homologous chromosomal sites throughout chromosomal arms enables DSB repair in a mech-

\* This work was supported by the Israel Science Foundation funded by the Academy of Sciences and Humanities and by the Minerva Foundation, Germany.

<sup>§</sup> This article contains supplemental Movies 1–6.

<sup>1</sup> To whom correspondence should be addressed. Tel.: 972-8-9342003; E-mail: avi.minsky@weizmann.ac.il.

<sup>2</sup> The abbreviations used are: DSB, double strand DNA break; NA, nalidixic acid; FROS, Fluorescent Repressor Operator Systems; eCFP, enhanced cyan fluorescent protein; eYFP, enhanced yellow fluorescent protein.

## Stress-induced Chromosome Pairing

anism that is independent of a genome-wide search yet consistent with the current physical understanding of the morphology of bacterial genomes. The results reported here imply that genome condensation, triggered even by relatively moderate stressful conditions and cellular damage, primes bacteria to rapidly and effectively cope with highly detrimental DNA lesions such as DSBs. Moreover, although our observations are consistent with the notion that RecA plays an essential role in the identification of accurate homologous template as well as in the formation of a stable complex between presynaptic filaments and their repair templates (2, 3, 36, 37), these findings imply that, in contrast to the widespread conviction, RecA-dependent genome-wide search is not required for DSB homologous repair.

### EXPERIMENTAL PROCEDURES

**Bacterial Strains and Growth Conditions (Table 1)**—*E. coli* wild-type strain used in this study was AB1157. WBN2 RecA<sup>−</sup> strain is an AB1157 derivative. IL05-RecA<sup>−</sup> was constructed by P1 transduction of the *DrecA306::Tn10* locus from WBN2 into IL05 and selection for tetracycline, gentamicin, and kanamycin resistance. The *recA* deletion was confirmed by colony PCR and DNA sequencing. A strain carrying I-SceI endonuclease under P<sub>BAD</sub> arabinose-inducible promoter and a single I-SceI chromosomal cut site (SMR8478; gift from S. Rosenberg) (1) was used for DSB induction at a single chromosomal site (Table 1). To construct the SMR8478-FseI strain (Table 1) that enables generation of five DSBs, plasmid pZS\*32-FseI that harbors FseI endonuclease under the control of the P<sub>LlacO-1</sub> promoter was transformed into SMR8478 cells. Cells were regularly grown in LB at 37 °C. NA and chloramphenicol (Sigma) were added to mid-log cultures to concentrations of 50–500 or 100 μg/ml, respectively. For endonuclease induction, SMR8478 and SMR8478-FseI strains were grown in M9 minimal medium supplemented with 0.1% glucose to A<sub>600</sub> = 0.3, centrifuged, resuspended in M9, including either 0.1% L-arabinose (for I-SceI induction) or 0.1% L-arabinose and 1 mM isopropyl 1-thio-β-D-galactopyranoside (for induction of both I-SceI and FseI endonucleases), and incubated at 37 °C for 1 h.

**Fluorescent Repressor Operator Systems (FROS) Studies (7, 12)**—*E. coli* strains IL05 (wild-type and RecA<sup>−</sup>) and WX51 were used for visualization of chromosomal sites. IL05 carries on its chromosome an array of 240 copies of *tetO* (*tetO240-Gm*) inserted close to the origin and an array of 240 copies of *lacO* (*lacO240-Km*) inserted close to the terminus site (Fig. 1A). A second strain for visualization of chromosomal sites, WX51, carries 240 copies of *lacO* and 240 copies of *tetO* inserted at 90° and 270° of the chromosome, respectively (Fig. 1B). A multicopy plasmid, pLAU53 (Table 1), expressing LacI-eCFP and TetR-eYFP (enhanced cyan and yellow fluorescent proteins, respectively) fusion repressors from P<sub>BAD</sub> arabinose promoter was used as a source of fluorescently labeled LacI and TetR. The FROS systems were kindly provided by D. Sherratt.

**Fluorescence Microscopy and Image Processing**—Strains were grown to A<sub>600</sub> ~0.5, treated with antibiotics, and stained with the membrane stain FM4-64 (25 μg/ml; Invitrogen) and DAPI (0.5 ng/ml; Sigma) for 15 min. For FROS experiments, *E. coli* IL05 (wild-type and RecA<sup>−</sup>) or WX51 carrying pLAU53 was

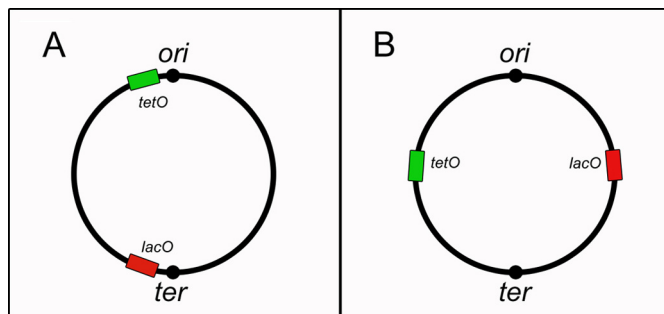


FIGURE 1. **FROS (7, 12).** A, FROS 1. *tetO* and *lacO* arrays were inserted close to the origin and terminal chromosomal sites, respectively (IL05 strain; Table 1). B, FROS 2. *lacO* and *tetO* arrays were inserted at 90° and 270° of the chromosome, respectively (WX51 strain; Table 1).

grown to A<sub>600</sub> ~0.3, induced with 0.01% L-arabinose for 30 min, and exposed to antibiotics as described above. Cells were then placed on 1% agarose pads prepared in a CoverWell Imaging Chamber (Sigma). Samples were visualized with ×100 oil immersion objective and photographed using a Deltavision microscope (Applied Precision). eCFP and eYFP were visualized by using ET470/24m and ET535/30m filters (Chroma), respectively. The signals of DAPI and FM4-64 were viewed by using ET457/40 and ET617/63 filters (Chroma), respectively. All images were identically de-convoluted and processed with the conservative SoftWorx package (Applied Precision).

Time-lapse studies were conducted on *E. coli* IL05 and WX51 cells carrying pLAU53. Cultures were grown in LB to A<sub>600</sub> ~0.3 and induced with 0.02% L-arabinose for 30 min. Cells were placed on 1% LB-agarose pads containing 500 μg/ml NA. Because of rapid bleaching of CFP, only YFP excitation was used in some time-lapse experiments, enabling localization of origin-proximal or 270° *tetO* foci. Images were de-convoluted with the conservative SoftWorx package and processed with ImageJ software.

### RESULTS

**Visualization of Chromosomal Sites**—Chromosomal site localization was analyzed by using *E. coli* strains in which *tetO* and *lacO* arrays were inserted at various chromosomal sites (Fig. 1). These strains carry a plasmid encoding TetR-eYFP and LacI-eCFP repressors (FROS) (7, 12). Decoration of chromosomal sites following replication with the fluorescently tagged repressors provides a means for probing cellular addresses of homologous sites located on sister chromosomes.

**Stressful Growth Conditions Result in a Nonrandom Genome Condensation and Convergence of Sister Chromosomes**—In unstressed, exponentially growing *E. coli* cells (strains IL05 and AB1157; Table 1), chromatin is spread over the entire cytoplasm (Fig. 2A; Table 2), as is the case for other bacterial strains such as *Bacillus subtilis* (29) and in archaea (33). In contrast and as previously shown (28), *E. coli* cells exposed to NA, a pleiotropic drug that inflicts diverse DNA lesions (nicks, gaps, and DSBs) (38, 39), reveal condensed chromatin morphology (Fig. 2B; Table 2). In addition, exposure of IL05 cells to oxidative irradiation (γ, <sup>137</sup>Cs source) that inflicts DNA lesions at doses of 100 and 200 gray resulted in genome condensation in 21 ± 2 and 34 ± 3% of the cells, respectively (data not shown). Notably,

**TABLE 1**  
Strains and plasmids

	Genotype	Source
<b>Strains</b>		
AB1157	<i>thr-1, araC14, leuB6(Am), Δ(gpt-proA)62, lacY1, tsx-33, qsr'-0, glnV44(AS), galK2(Oc), LAM-, Rac-0, hisG4(Oc), rfbC1, mgl-51, rpoS396(Am), rpsL31(strR), kdgK51, xylA5, mtl-1, argE3(Oc), thi-1</i>	
WBN2	RecA <sup>-</sup> (AB1157 ( $\Delta$ RecA306::Tn10))	
IL05	AB1157 ( <i>lacO240-Km</i> ]1801; <i>tetO240-Gm</i> ]3908.	7, 12
WX51	AB1157 ( <i>lacO240-Km</i> at 90° and <i>tetO240-Gm</i> at 270°)	7, 12
IL05-RecA <sup>-</sup>	IL05 ( $\Delta$ RecA306::Tn10)	This study
SMR8478	MG1655 ( $\Delta$ attλ::P <sub>sulA</sub> Ωgfp-mut2 attP21::pAH81-P <sub>BAD</sub> ΩI-SceI)	1
SMR8478-FseI	MG1655 ( $\Delta$ attλ::P <sub>sulA</sub> Ωgfp-mut2 attP21::pAH81-P <sub>BAD</sub> ΩI-SceI::pZS*32-FseI)	This study
<b>Plasmids</b>		
pLAU53	pUC18 derivative containing genes for fusion proteins LacI-eCFP and TetR-eYFP under <i>ara</i> promoter	7, 12
pZS*32-MCS	pZ vector system	This study
pZS*32-FseI	FseI endonuclease under P <sub>LacO-1</sub> promoter	This study

genotoxic stress was also shown to elicit genome condensation in *B. subtilis* (29) and archaea (33).

To locate specific chromosomal sites following stress-induced genome condensation, we used IL05 *E. coli* strain (Table 1), in which *tetO* and *lacO* arrays were inserted near the replication origin and chromosomal terminus, respectively (FROS 1; Fig. 1A) (7). Unstressed exponentially growing IL05 cells reveal two or four origin-proximal sites but only one terminus-proximal site (Fig. 2, C, E, G, and I), in keeping with multifork replication and rapid chromosome segregation (7, 12, 13, 40). In sharp contrast, NA-treated cells reveal only a single origin-proximal focus or two closely adjacent foci (Fig. 2, D, F, H, and J; Tables 3 and 4), which are always separated from the terminus-proximal site. These observations are supported by time-lapse experiments (supplemental Movies S1 and S2), which reveal progressive convergence of origin-proximal sites that culminates in their coalescence. Notably, whereas the inherently limited resolution of fluorescence microscopy does not allow unequivocal determination of the precise relative position of the origin-proximal foci, the progressive approach of these sites toward each other as well as the observation that once merged they remain co-localized support the notion that these foci do indeed coalesce. Collectively, these findings indicate co-localization of homologous sites (represented by origin-proximal foci) but not of nonhomologous sites (origin- and terminus-proximal sites).

We propose that this co-localization of chromosomal homologous sites results from the convergence of sister chromosomes. A single origin-proximal focus in NA-treated bacteria derives from cells that, prior to being exposed to stress, maintained a single pair of segregating sister chromosomes that originated from a single replication-firing event. Two contiguous origin-proximal foci are suggested to arise from the convergence of two pairs of chromosome arms that resulted from two successive replication-firing events (as indicated in the model depicted in Fig. 6). This conjecture, which is supported by our time-lapse movies (supplemental Movies S1–S6), is further substantiated by a statistical analysis conducted on a large number (>500) of unstressed and NA-exposed cells. This analysis demonstrated that in unstressed cells, the ratio between two and four origin-proximal foci is 0.41. This ratio is very similar to that of a single and two contiguous foci revealed in NA-treated cells (0.44), implying that chromosome convergence occurs

between chromosome sisters that derive from an identical replication-firing event. Notably, NA removal results in a progressive increase in the number of fluorescent foci in a limited but significant cell population (Table 5), indicating reversibility of genome condensation and re-initiation of chromosome segregation.

To corroborate the claim that stress-induced genome condensation promotes convergence of sister chromosomes and to eliminate the possibility that this convergence is limited to origin-proximal sites, we used an additional FROS strain (WX51; Table 1) in which *lacO* and *tetO* arrays were inserted at 90° and 270° sites of the chromosome, respectively (FROS 2; Fig. 1B) (12). Exponentially growing cells reveal two or four *tetO* and *lacO* foci (Fig. 3, A, C, and E; Table 6) that, following NA treatment, merge into a single *tetO* and a single *lacO* foci that are always spatially separated (Fig. 3, B, D, and F). Whereas only the *tetO* array (270° chromosomal site) could be probed in time-lapse experiments due to rapid eCFP bleaching, studies on cells fixed at different time points revealed that the nonhomologous *tetO* and *lacO* foci are consistently spatially separated, as shown in Fig. 3B. Notably, because FROS 2 probes the location of two distinct chromosomal sites, these observations, corroborated by time-lapse experiments (Fig. 3, C–F; supplemental Movie S3), further support the notion that genome condensation promotes convergence of chromosome arms throughout their entire length.

*Insights from Induction of Double Strand DNA Breaks at Precise Number and Chromosomal Sites*—The DNA-damaging agents described above (NA, oxidative irradiation) inflict lesions at random chromosomal sites and at a frequency that cannot be precisely controlled. We therefore sought to examine the correlation between genome condensation and generation of DNA lesions at a well defined number and at specific chromosomal sites.

Toward this aim, we used an *E. coli* strain (SMR8478) that carries the inducible double strand I-SceI endonuclease and a single I-SceI cut site, thus enabling the generation of a single DSB at a specific chromosomal site (1). Whereas induction of I-SceI was shown to generate a DSB in a large majority of the cells (1), such induction resulted in genome condensation in only a small percentage of the population ( $6 \pm 1\%$ ; 88 cells probed in two experiments) (data not shown). In light of the fact that the I-SceI cut site is located near the origin of replication

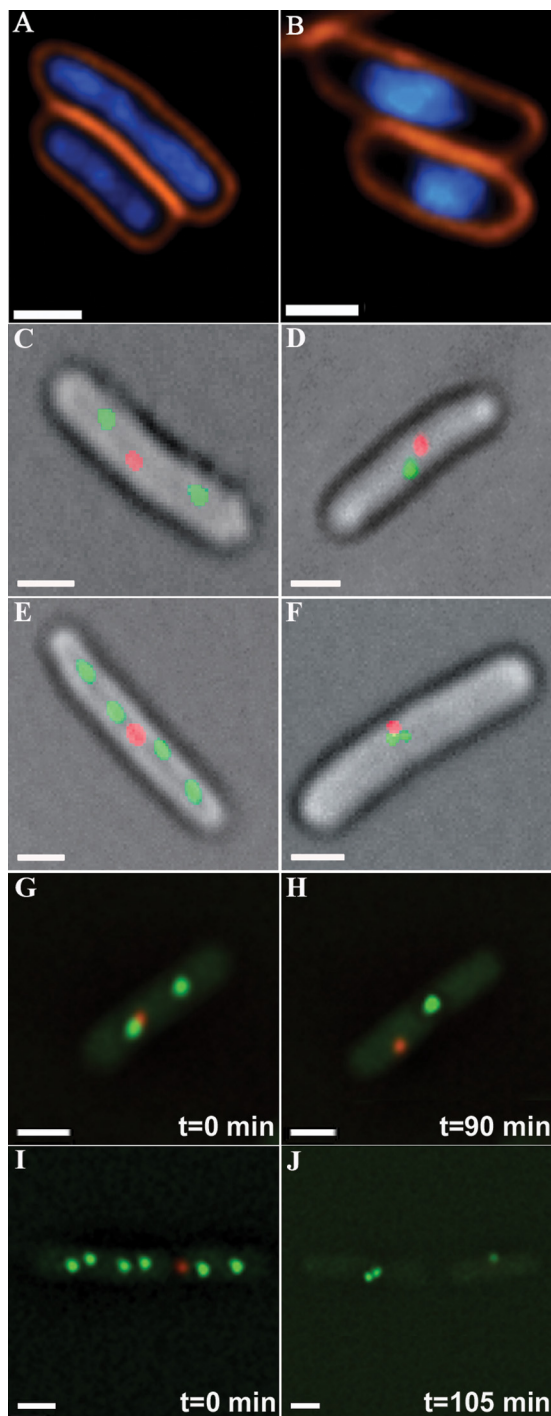


**FIGURE 2. Chromosomal organization and site localization in *E. coli* (FROS 1) exposed to NA.** *A*, expanded genomes in unstressed cells. *B*, genome condensation following exposure to NA (1 h; 350  $\mu\text{g/ml}$ ) (DNA stained blue with DAPI, and cell membranes stained orange with FM4-64). *C*, *E*, *G*, and *I*, unstressed cells carrying FROS 1 (Fig. 1A) reveal two or four origin-proximal foci (green) and a single terminus-proximal focus (red). *D*, *F*, *H*, and *J*, following NA treatment, two foci coalesce into a single focus, and four foci merge into two adjacent foci. *G*, *I*, *H*, and *J* are initial and final frames from time-lapse experiments (supplemental Movies S1 and S2, respectively). Notably, two cells are depicted in *I* and *J*. Scale bars, 0.5  $\mu\text{m}$ .

(355,395 bp from the origin in an  $\sim 4,700$ -kbp chromosome site (1)), we suggest that the low extent of genome condensation reflects the fact that in most cells endonuclease induction occurred when replication forks have already proceeded

**TABLE 2**  
Effects of NA on DNA condensation in WT *E. coli* (AB1157)

NA <sup>a</sup>	Spread genome	Condensed genome	n/N <sup>b</sup>
$\mu\text{g/ml}$	% of cells	% of cells	
0	97 $\pm$ 2	3 $\pm$ 2	680/6
100	7 $\pm$ 2	93 $\pm$ 2	492/6
350	2 $\pm$ 2	98 $\pm$ 2	486/6
500	0	99 $\pm$ 2	703/6

<sup>a</sup> Exposure time was 60 min.

<sup>b</sup> n in all tables represents the total number of cells scored for a given set of conditions. N is the number of independent experiments conducted.

**TABLE 3**  
Effects of NA (100  $\mu\text{g/ml}$ ) on the distribution of origin-proximal homologous sites in *E. coli* IL05

NA incubation	1 focus	2 adjacent foci	$\geq 2$ separated foci	n/N
min	% of cells	% of cells	% of cells	
0	0	2 $\pm$ 1	98 $\pm$ 1	330/3
10	3 $\pm$ 1	4 $\pm$ 1	93 $\pm$ 1	178/3
20	14 $\pm$ 3	18 $\pm$ 3	68 $\pm$ 3	102/2
40	33 $\pm$ 3	37 $\pm$ 3	30 $\pm$ 3	304/3
60	43 $\pm$ 3	48 $\pm$ 3	9 $\pm$ 3	315/3

**TABLE 4**  
Effects of NA (350  $\mu\text{g/ml}$ ) on the distribution of origin-proximal homologous sites in *E. coli* IL05

NA incubation	1 focus	2 adjacent foci	$\geq 2$ separated foci	n/N
min	% of cells	% of cells	% of cells	
10	5 $\pm$ 3	5 $\pm$ 3	90 $\pm$ 3	151/2
20	18 $\pm$ 2	20 $\pm$ 2	63 $\pm$ 2	176/2
40	38 $\pm$ 4	39 $\pm$ 4	23 $\pm$ 4	244/3
60	46 $\pm$ 2	51 $\pm$ 2	3 $\pm$ 2	375/3

**TABLE 5**  
Distribution of origin-proximal sites following NA (100  $\mu\text{g/ml}$ ) removal

Time following NA removal	1 focus	2 foci	n/N
min	% of cells	% of cells	
0	85 $\pm$ 5	15 $\pm$ 5	71/3
30	68 $\pm$ 5	32 $\pm$ 5	122/3
60	64 $\pm$ 6	36 $\pm$ 6	55/2

through the I-SceI site and consequently is not affected by this lesion.

To verify this conjecture, we constructed a strain (SMR8478-FseI; Table 1) that enables infliction of four double strand DNA breaks at natively present FseI sites, in addition to the single DSB generated by the I-SceI endonuclease. Induction of both I-SceI and FseI, which generates five DSBs, resulted in genome condensation in 32  $\pm$  2% of the cells (260 cells probed in three different experiments). We claim that this substantial increase in the population of cells that undergo genome condensation following infliction of five DSBs is consistent with the notion that generation of DNA lesions, the ensuing stalling of replication forks, and genome condensation are mechanistically related.

*RecA and DSBs Are Required for Persistent Co-localization of Sister Chromosomes and Homologous Sites*—To gain deeper insights into the mechanistic implications of stress-mediated genome condensation and chromosomal arm convergence, we studied these processes in two *E. coli* strains deficient in the recombination-repair protein RecA (WBN2 and IL05-RecA<sup>-</sup>;

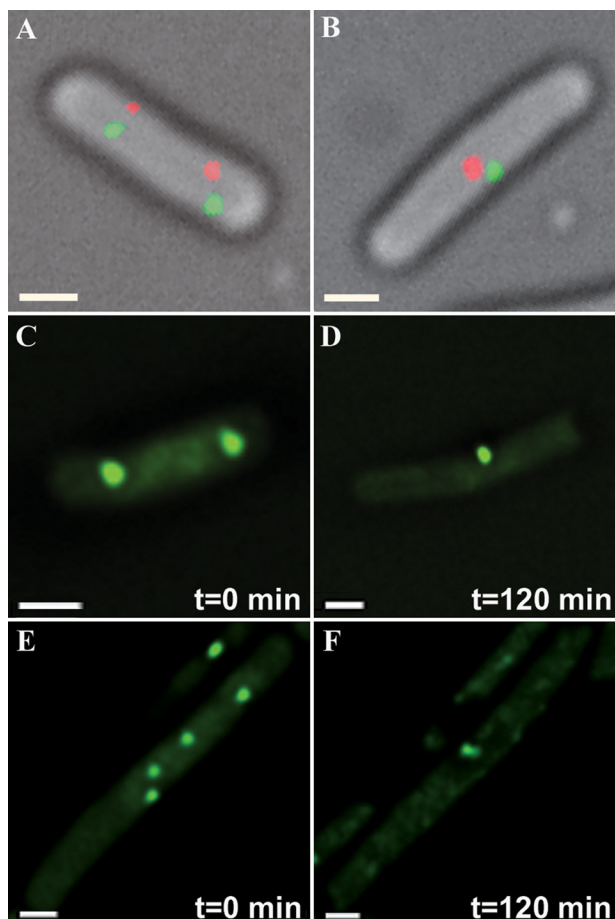


**FIGURE 3. Chromosomal site localization in *E. coli* (FROS 2) exposed to NA.** A, C, and E, distribution of chromosomal foci in nonstressed *E. coli* cells carrying FROS 2 (Fig. 1B). B, D, and F, cells exposed to NA, revealing co-localization of homologous but not of nonhomologous sequences (red and green foci). C–F (supplemental Movie S3) represent the initial and final frames from time-lapse experiments. In the time-lapse studies only the *tetO* array (270° chromosomal site) was probed due to rapid eCFP bleaching. Scale bars, 0.5  $\mu\text{m}$ .

**TABLE 6**  
Effects of NA (350  $\mu\text{g}/\text{ml}$ ) on the distribution of site located at 270° of the chromosome in *E. coli* WX51

Similar results were obtained for the chromosomal site at 90°.

NA incubation	1 focus	2 contiguous foci	$\geq 2$ foci	n/N
min	% of cells	% of cells	% of cells	
0	7 $\pm$ 0.5	0	93 $\pm$ 0.5	364/3
30	60 $\pm$ 2	12 $\pm$ 2	28 $\pm$ 2	514/3
60	81 $\pm$ 2	12 $\pm$ 2	7 $\pm$ 2	499/4

Table 1). Exposure of these strains to low NA doses resulted in genome condensation in a limited fraction of the bacterial population (Table 7), in keeping with previous observations demonstrating that RecA promotes genome condensation (28). Higher NA concentrations triggered condensation in a significantly larger population (Fig. 4, A and B; Table 7). Following exposure to such doses, convergence of origin-proximal sites into close spatial proximity was detected in 68 out of 80 cells (85%). However, and in clear contrast to wild-type cells, convergence did not result in persistent co-localization of homologous sites but rather in two adjacent foci or a single focus that, in most cases, subsequently segregated into two closely apposed

**TABLE 7**  
Effects of NA on DNA packaging in RecA<sup>-</sup> *E. coli* (WBN2)

NA <sup>a</sup>	Fully spread genome	Condensed genome	n/N
$\mu\text{g}/\text{ml}$	% of cells	% of cells	
0	93 $\pm$ 2	7 $\pm$ 2	101/6
100	68 $\pm$ 5	32 $\pm$ 5	744/4
350	42 $\pm$ 3	58 $\pm$ 3	490/4
500	11 $\pm$ 0.5	89 $\pm$ 0.5	470/3

<sup>a</sup> Exposure time was 60 min.

foci (Fig. 4, C–G; supplemental Movies S4 and S5). These results indicate that, although genome condensation and sister chromosome convergence may occur in the absence of RecA, persistent sister co-localization is RecA-dependent. This observation is consistent with the fact that RecA is required for the formation of a lasting complex between presynaptic filaments generated at DSB sites and their homologous repair partners (2, 3).

Similar results were obtained when wild-type IL05 cells were exposed to chloramphenicol, an antibiotic that inhibits protein synthesis. As shown previously, chloramphenicol treatment results in chromatin condensation into toroidal structures (Fig. 5A) (41). Time-lapse studies in which 60 cells were probed following exposure to chloramphenicol revealed that in 52 cells (86.6%) homologous origin-proximal sites converged into close vicinity or merged into a single focus that then segregated into two closely apposed foci (Fig. 5, B–D; supplemental Movie S6). Because chloramphenicol does not inflict DNA lesions, these observations imply that DSBs are not required for sister chromosome convergence yet are essential for stabilizing their co-localization through the formation of robust and persistent presynaptic filaments-homologous template-RecA joint complexes, as is the case for RecA (2, 3).

## DISCUSSION

This study was motivated by two considerations. The first is the increasing realization that exposure of bacteria to diverse stressful conditions, including starvation (27, 42), UV irradiation (28, 29), various antibiotics (31), and oxidative stress (32), results in massive genome condensation. Whereas this apparently generic stress response was previously proposed to promote DNA protection through physical sequestration (27, 43, 44) or to predispose bacteria to programmed cell death (31), the physiological implications of this process remain unclear. The second consideration was the unlikelihood of homologous repair pathways of double strand DNA breaks that rely on genome-wide search conducted by DNA ends for their repair templates. As indicated in the Introduction, such a search is inconsistent with the highly restricted motility of chromosomal sites, which is reflected by their precise and persistent localization at particular cytoplasmic addresses. The enigmatic nature of a genome-wide homology search has indeed been repeatedly highlighted (24). Intriguingly, studies conducted on yeast cells revealed an increased mobility of chromosomal sites following induction of DSBs and proposed that this enhanced motility promotes homology search (45, 46). A recent study (also conducted on yeast) demonstrated, however, that an *a priori* proximity between homologous sites, imposed by nuclear architectural features such as telomere and centromere clustering, plays

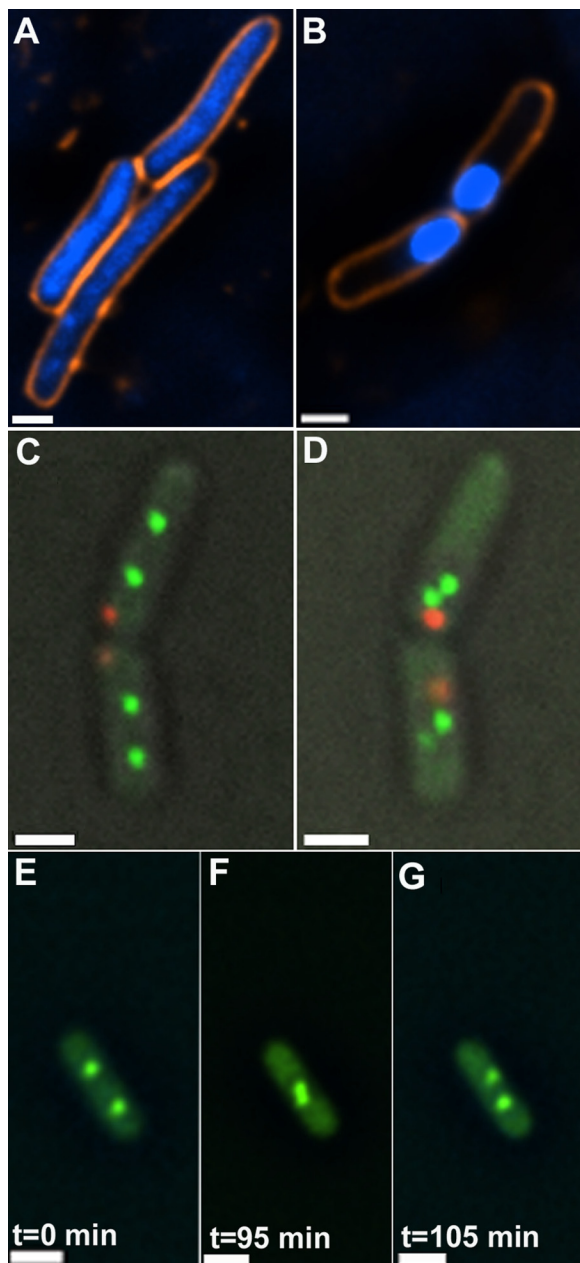


FIGURE 4. **Genome organization and chromosomal foci in RecA<sup>-</sup> cells exposed to NA.** *A*, genomes in untreated cells. *B*, genome condensation following NA treatment. *C* and *D*, cells at time 0 (*C*) and following 120 min of exposure to NA (*D*) reveal convergence, but not co-localization, of origin-proximal (green) sites. *E–G*, frames from supplemental Movie S4 showing co-localization and subsequent separation of origin-proximal foci. Scale bars, 0.5  $\mu$ m.

a crucial role in enhancing the efficiency of DSB homologous repair (47).

Previous studies revealed that condensation of bacterial genome is mediated by specific stress-induced DNA-binding proteins such as Dps during starvation (27, 42) or RecA following infliction of DNA damage (28, 29). The observations reported here, according to which genome condensation occurs in RecA<sup>-</sup> cells as well as in wild-type bacteria in which protein synthesis is inhibited, imply that condensation can be induced through an alternative, generic, pathway. This notion is corroborated by recent observations according to which exposure of bacteria to oxidative stress results in genome pack-

aging in a process that is independent of the main DNA-binding structural proteins such as Dps, H-NS, IHF, HU, and MukB (32).

Genome morphology in bacteria has been argued to represent a balance between the ever-present condensing factors that include the highly crowded cellular environment as well as attractive DNA-DNA interactions (48–51) and the expanding factors associated with metabolic activities (52, 53). These consist of DNA replication, transcription, chromosome segregation and, in particular, coupled transcription-translation and membrane insertion of membrane proteins that occur in bacteria (54). Indeed, a recent study demonstrated that expression of membrane proteins plays a crucial role in maintaining an expanded conformation of bacterial chromosomes (55). Collectively, these considerations imply that attenuated metabolic activity imposed by diverse stressful conditions such as starvation, drug-induced inhibition of protein synthesis, or exposure to DNA-damaging agents (previously demonstrated to induce replication arrest and cell cycle arrest by stalling replication forks (3, 56)) triggers DNA condensation. This condensation is presumably effected by tipping the balance between genome expansion and condensation toward the latter, as suggested previously (30, 57, 58).

On the basis of these considerations and the observations described above, we propose that stress-induced genome condensation maintains a crucial and heretofore unconsidered role in repair of bacterial DSBs. Specifically, we show that condensation does not proceed through random DNA collapse but rather through an orderly convergence and realignment of sister chromosomes throughout their length (Fig. 6). We suggest that this convergence is mediated by the long hypothesized (50, 59, 60) and recently *in vitro* demonstrated (34, 35, 61, 62) ability of identical (homologous) double-stranded DNA molecules to specifically identify each other and to generate relatively robust complexes. Significantly, this process was shown to be protein-independent and to be promoted by DNA condensation (35, 60, 63). We further propose that chromosome-realignment mediated by homologous dsDNA-dsDNA interactions is initiated at replication forks where  $\sim 300,000$  bp of the newly replicated sisters remain apposed before segregation is initiated (14). Such *a priori* paired regions may act as nucleation sites for convergence of the remaining sections of the sister chromosomes that then proceed sequentially in a zipper-like manner.

The conjecture that genome condensation and a nonrandom re-pairing of sister chromosomes are initiated at replication forks is supported by the results derived from the induction of DSBs by endonucleases, which imply that DNA lesions inflicted at sites that have already been replicated and as such do not encounter replication forks do not induce DNA packaging. This proposal is also corroborated by our time-lapse experiments, which reveal that two homologous sites merge into a single fluorescent focus whereas four sites, present on two pairs of homologous chromosomal arms, coalesce into two foci (as depicted in Fig. 6). It is further supported by our finding that the ratio between two and four fluorescent foci in unstressed cells is similar to the ratio between a single and two foci in NA-exposed cells, implying that a single pair of segregating chromosomes converges into a single focus (Fig. 6A), whereas two pairs of

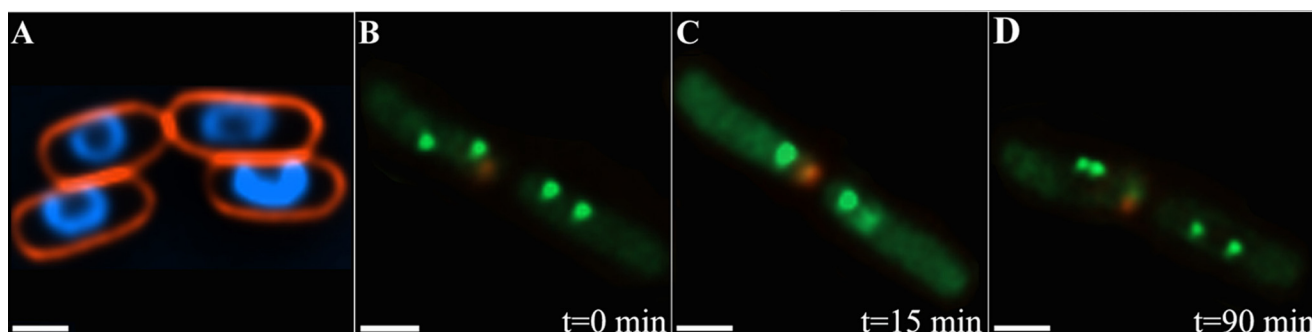


FIGURE 5. **Effects of chloramphenicol on chromosomal foci localization.** *A*, chromatin packaging into toroidal structures following exposure of IL05 to chloramphenicol. *B–D*, frames from a time-lapse experiment (supplemental Movie 6) in which IL05 cells were exposed to 150  $\mu\text{g/ml}$  chloramphenicol, depicting merging followed by separation of homologous, origin-proximal foci in the right-side of the cell, and foci convergence followed by segregation in the left-side of the cell. Scale bars, 1.0  $\mu\text{m}$  in *A*, and 0.5  $\mu\text{m}$  in *B–D*.

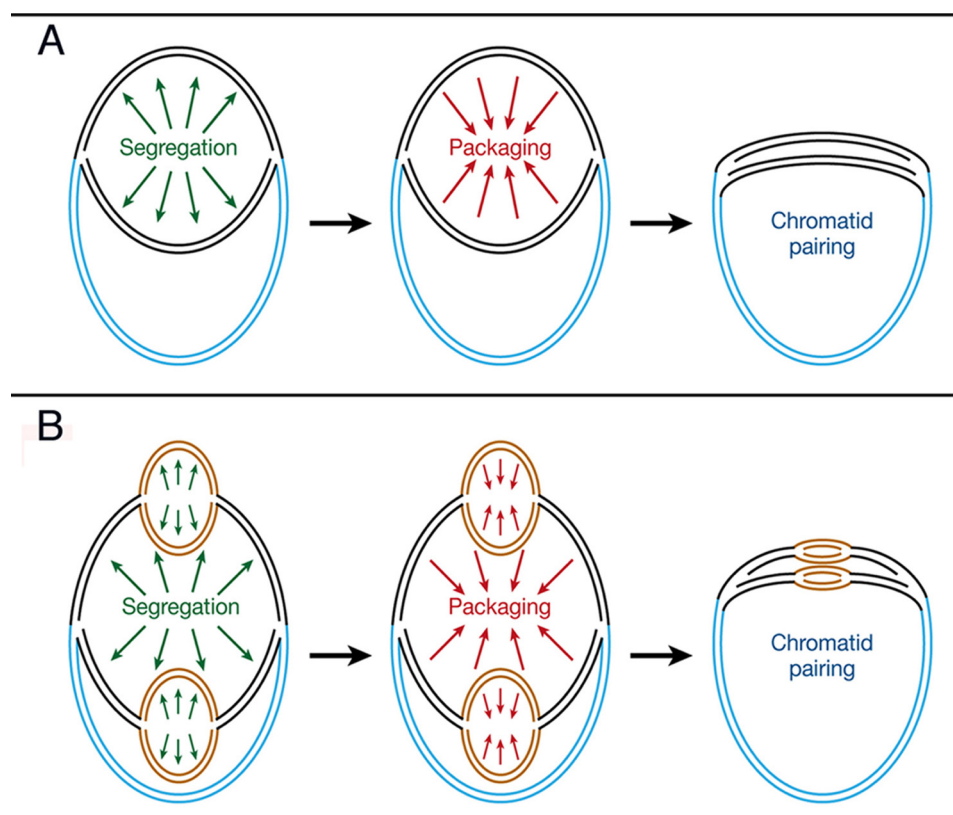


FIGURE 6. **Schematic model of stress-induced convergence of chromosomal arms.** Growing bacteria reveal either one (*A*) or two (*B*) pairs of newly replicated chromosome arms (black and brown ribbons, respectively). Adverse growth conditions promote genome condensation and sister chromosome convergence, which is initiated at the replication forks that act as nucleation sites and proceed in a zipper-like pathway. The resulting spatial proximity of homologous sites throughout chromosome arms enables interaction of DSBs with their homologous templates in a process that relies on random, short range, and diffusion-driven collisions rather than on a genome-wide homologous search.

chromosome arms that result from two successive replication-firing events merge into two adjacent foci (Fig. 6*B*).

Following chromosome arm convergence, homologous sites on both arms are brought into close spatial proximity throughout the chromosome arms (Fig. 6). We suggest that this proximity enables DSBs to find their homologous repair templates through short range diffusion-driven random collisions that were shown to govern genomic DNA motion (23). Notably, although such a spatially constrained motion is incompatible with a genome-wide search, it is consistent with the notion that the main recombination protein RecA is not required for the homology search. RecA is, however, essential for accurate

homology recognition and the subsequent formation of a stable recombination synapse (2, 3). This claim is supported by the finding that in  $\text{RecA}^-$  cells exposed to NA, homologous sites converge but do not form lastingly co-localized foci. It is also consistent with the observation that in chloramphenicol-treated wild-type cells, chromosome arms converge but do not merge into lasting foci, as DSBs, along with RecA, are required for the formation of a robust joint recombination complex between presynaptic filaments and their homologous templates (2, 3).

It has been proposed that chromatid cohesion in eukaryotes evolved to enable DNA repair (4) and is, accordingly, enhanced

## Stress-induced Chromosome Pairing

following infliction of DSBs (5, 64). This notion, along with the bacterial DSB repair pathway proposed here, implies that the *a priori* juxtaposition of homologous partners is a critical prerequisite for homologous repair of DSBs, a prerequisite that is conserved in bacteria and eukaryotes. An intriguing implication is that genome condensation and chromosome re-pairing effected by diverse stressful conditions prime bacteria to rapidly and effectively cope with highly detrimental DNA lesions by facilitating homologous repair of DSBs. Moreover, by implying that stress-induced DNA condensation is initiated at replication forks, the observations presented here support the notion (65–71) that homologous recombination evolved mainly to repair stalled replication forks, rather than to generate genetic diversity. An additional corollary of this study is that the innate physicochemical properties of DNA molecules, including their tendency to condense under appropriate conditions and the ability of identical double-stranded DNA molecules to identify each other and generate a robust complex, are directly pertinent to their physiological activities (43, 49, 57, 72, 73).

---

*Acknowledgments*—We thank D. Sherratt for providing systems for chromosomal site localization and D. Ben-Halevy, G. Haran, Z. Livneh, and Y. Mutsafi for helpful comments. Fluorescence studies were conducted at the Moskowitz Center for Bio-Nano Imaging at the Weizmann Institute of Science.

---

### REFERENCES

1. Pennington, J. M., and Rosenberg, S. M. (2007) Spontaneous DNA breakage in single living *Escherichia coli* cells. *Nat. Genet.* **39**, 797–802
2. Kowalczykowski, S. C., Dixon, D. A., Eggleston, A. K., Lauder, S. D., and Rehrauer, W. M. (1994) Biochemistry of homologous recombination in *Escherichia coli*. *Microbiol. Rev.* **58**, 401–465
3. Kuzminov, A. (1999) Recombinational repair of DNA damage in *Escherichia coli* and bacteriophage  $\lambda$ . *Microbiol. Mol. Biol. Rev.* **63**, 751–813
4. Sjögren, C., and Nasmyth, K. (2001) Sister chromatid cohesion is required for postreplicative double strand break repair in *Saccharomyces cerevisiae*. *Curr. Biol.* **11**, 991–995
5. Ström, L., Karlsson, C., Lindroos, H. B., Wedahl, S., Katou, Y., Shirahige, K., and Sjögren, C. (2007) Postreplicative formation of cohesion is required for repair and induced by a single DNA break. *Science* **317**, 242–245
6. Unal, E., Heidinger-Pauli, J. M., and Koshland, D. (2007) DNA double strand breaks trigger genome-wide sister-chromatid cohesion through Eco1 (Ctf7). *Science* **317**, 245–248
7. Lau, I. F., Filipe, S. R., Soballe, B., Økstad, O. A., Barre, F. X., and Sherratt, D. J. (2003) Spatial and temporal organization of replicating *Escherichia coli* chromosomes. *Mol. Microbiol.* **49**, 731–743
8. Sherratt, D. J. (2003) Bacterial chromosome dynamics. *Science* **301**, 780–785
9. Viollier, P. H., Thanbichler, M., McGrath, P. T., West, L., Meewan, M., McAdams, H. H., and Shapiro, L. (2004) Rapid and sequential movement of individual chromosomal loci to specific subcellular locations during bacterial DNA replication. *Proc. Natl. Acad. Sci. U.S.A.* **101**, 9257–9262
10. Nielsen, H. J., Ottesen, J. R., Youngren, B., Austin, S. J., and Hansen, F. G. (2006) The *Escherichia coli* chromosome is organized with the left and right chromosome arms in separate cell halves. *Mol. Microbiol.* **62**, 331–338
11. Nielsen, H. J., Youngren, B., Hansen, F. G., and Austin, S. (2007) Dynamics of *Escherichia coli* chromosome segregation during multifork replication. *J. Bacteriol.* **189**, 8660–8666
12. Wang, X., Liu, X., Possoz, C., and Sherratt, D. J. (2006) The two *Escherichia coli* chromosome arms locate to separate cell halves. *Genes Dev.* **20**, 1727–1731
13. Reyes-Lamothe, R., Possoz, C., Danilova, O., and Sherratt, D. J. (2008) Independent positioning and action of *Escherichia coli* replisomes in live cells. *Cell* **133**, 90–102
14. Joshi, M. C., Bourniquel, A., Fisher, J., Ho, B. T., Magnan, D., Kleckner, N., and Bates, D. (2011) *Escherichia coli* sister chromosome separation includes an abrupt global transition with concomitant release of late-splitting intersister snaps. *Proc. Natl. Acad. Sci. U.S.A.* **108**, 2765–2770
15. Teleman, A. A., Graumann, P. L., Lin, D. C., Grossman, A. D., and Losick, R. (1998) Chromosome arrangement within a bacterium. *Curr. Biol.* **8**, 1102–1109
16. Niki, H., Yamaichi, Y., and Hiraga, S. (2000) Dynamic organization of chromosomal DNA in *Escherichia coli*. *Genes Dev.* **14**, 212–223
17. Thanbichler, M., Wang, S. C., and Shapiro, L. (2005) The bacterial nucleoid: A highly organized and dynamic structure. *J. Cell. Biochem.* **96**, 506–521
18. Thanbichler, M., and Shapiro, L. (2008) Getting organized—how bacterial cells move proteins and DNA. *Nat. Rev. Microbiol.* **6**, 28–40
19. White, M. A., Eykelenboom, J. K., Lopez-Vernaza, M. A., Wilson, E., and Leach, D. R. (2008) Nonrandom segregation of sister chromosomes in *Escherichia coli*. *Nature* **455**, 1248–1250
20. Montero Llopis, P., Jackson, A. F., Sliusarenko, O., Surovtsev, I., Heinritz, J., Emonet, T., and Jacobs-Wagner, C. (2010) Spatial organization of the flow of genetic information in bacteria. *Nature* **466**, 77–81
21. Postow, L., Hardy, C. D., Arsuaiga, J., and Cozzarelli, N. R. (2004) Topological domain structure of the *Escherichia coli* chromosome. *Genes Dev.* **18**, 1766–1779
22. Boccard, F., Esnault, E., and Valens, M. (2005) Spatial arrangement and macrodomain organization of bacterial chromosomes. *Mol. Microbiol.* **57**, 9–16
23. Marshall, W. F., Straight, A., Marko, J. F., Swedlow, J., Dernburg, A., Belmont, A., Murray, A. W., Agard, D. A., and Sedat, J. W. (1997) Interphase chromosomes undergo constrained diffusional motion in living cells. *Curr. Biol.* **7**, 930–939
24. Weiner, A., Zauberman, N., and Minsky, A. (2009) Recombinational DNA repair in a cellular context: a search for the homology search. *Nat. Rev. Microbiol.* **7**, 748–755
25. Chen, Z., Yang, H., and Pavletich, N. P. (2008) Mechanism of homologous recombination from the RecA-ssDNA/dsDNA structures. *Nature* **453**, 489–494
26. De Vlaminck, I., van Loenhout, M. T., Zweifel, L., den Blanken, J., Hooning, K., Hage, S., Kerssemakers, J., and Dekker, C. (2012) Mechanism of homology recognition in DNA recombination from dual-molecule experiments. *Mol. Cell* **46**, 616–624
27. Wolf, S. G., Frenkiel, D., Arad, T., Finkel, S. E., Kolter, R., and Minsky, A. (1999) DNA protection by stress-induced biocrystallization. *Nature* **400**, 83–85
28. Levin-Zaidman, S., Frenkiel-Krispin, D., Shimoni, E., Sabanay, I., Wolf, S. G., and Minsky, A. (2000) Ordered intracellular RecA-DNA assemblies: a potential site of *in vivo* RecA-mediated activities. *Proc. Natl. Acad. Sci. U.S.A.* **97**, 6791–6796
29. Smith, B. T., Grossman, A. D., and Walker, G. C. (2002) Localization of UvrA and effect of DNA damage on the chromosome of *Bacillus subtilis*. *J. Bacteriol.* **184**, 488–493
30. Cook, P. R. (2002) Predicting three-dimensional genome structure from transcriptional activity. *Nat. Genet.* **32**, 347–352
31. Dwyer, D. J., Camacho, D. M., Kohanski, M. A., Callura, J. M., and Collins, J. J. (2012) Antibiotic-induced bacterial cell death exhibits physiological and biochemical hallmarks of apoptosis. *Mol. Cell* **46**, 561–572
32. Ko, K. C., Tai, P. C., and Derby, C. D. (2012) Mechanisms of action of escapin, a bactericidal agent in the ink secretion of the sea hare *Aplysia californica*: Rapid and long-lasting DNA condensation and involvement of the OxyR-regulated oxidative stress pathway. *Antimicrob. Agents Chemother.* **56**, 1725–1734
33. Delmas, S., Duggin, I. G., and Allers, T. (2013) DNA damage induces nucleoid compaction via the Mre11-Rad50 complex in the archaeon *Haloflex volcanii*. *Mol. Microbiol.* **87**, 168–179



34. Baldwin, G. S., Brooks, N. J., Robson, R. E., Wynveen, A., Goldar, A., Leikin, S., Seddon, J. M., and Kornyshev, A. A. (2008) DNA double helices recognize mutual sequence homology in a protein free environment. *J. Phys. Chem. B* **112**, 1060–1064
35. Danilowicz, C., Lee, C. H., Kim, K., Hatch, K., Coljee, V. W., Kleckner, N., and Prentiss, M. (2009) Single molecule detection of direct, homologous, DNA/DNA pairing. *Proc. Natl. Acad. Sci. U.S.A.* **106**, 19824–19829
36. Szostak, J. W., Orr-Weaver, T. L., Rothstein, R. J., and Stahl, F. W. (1983) The double strand-break repair model for recombination. *Cell* **33**, 25–35
37. Folta-Stogniew, E., O'Malley, S., Gupta, R., Anderson, K. S., and Radding, C. M. (2004) Exchange of DNA base pairs that coincides with recognition of homology promoted by *E. coli* RecA protein. *Mol. Cell* **15**, 965–975
38. Reece, R. J., and Maxwell, A. (1991) DNA gyrase: structure and function. *Crit. Rev. Biochem. Mol. Biol.* **26**, 335–375
39. Bejerano-Sagie, M., Oppenheimer-Shaanan, Y., Berlatzky, I., Rouvinski, A., Meyerovich, M., and Ben-Yehuda, S. (2006) A checkpoint protein that scans the chromosome for damage at the start of sporulation in *Bacillus subtilis*. *Cell* **125**, 679–690
40. Nielsen, H. J., Li, Y., Youngren, B., Hansen, F. G., and Austin, S. (2006) Progressive segregation of the *Escherichia coli* chromosome. *Mol. Microbiol.* **61**, 383–393
41. Zimmerman, S. B. (2002) Toroidal nucleoids in *Escherichia coli* exposed to chloramphenicol. *J. Struct. Biol.* **138**, 199–206
42. Frenkiel-Krispin, D., Levin-Zaidman, S., Shimoni, E., Wolf, S. G., Wachtel, E. J., Arad, T., Finkel, S. E., Kolter, R., and Minsky, A. (2001) Regulated phase transitions of bacterial chromatin: a nonenzymatic pathway for generic DNA protection. *EMBO J.* **20**, 1184–1191
43. Minsky, A. (2004) Information content and complexity in the high-order organization of DNA. *Annu. Rev. Biophys. Biomol. Struct.* **33**, 317–342
44. Frenkiel-Krispin, D., and Minsky, A. (2006) Nucleoid organization and the maintenance of DNA integrity in *E. coli*, *B. subtilis* and *D. radiodurans*. *J. Struct. Biol.* **156**, 311–319
45. Miné-Hattab, J., and Rothstein, R. (2012) Increased chromosome mobility facilitates homology search during recombination. *Nat. Cell Biol.* **14**, 510–517
46. Dion, V., Kalck, V., Horigome, C., Towbin, B. D., and Gasser, S. M. (2012) Increased mobility of double strand breaks requires Mec1, Rad9 and the homologous recombination machinery. *Nat. Cell Biol.* **14**, 502–509
47. Renkawitz, J., Lademann, C. A., Kalocsay, M., and Jentsch, S. (2013) Monitoring homology search during DNA double strand break repair *in vivo*. *Mol. Cell* **50**, 261–272
48. Gronbech-Jensen, N., Mashl, R. J., Bruinsma, R. F., and Gelbart, W. M. (1997) Counterion-induced attraction between rigid polyelectrolytes. *Phys. Rev. Lett.* **78**, 2477–2480
49. Strey, H. H., Podgornik, R., Rau, D. C., and Parsegian, V. A. (1998) DNA-DNA interactions. *Curr. Opin. Struct. Biol.* **8**, 309–313
50. Kornyshev, A. A., and Leikin, S. (1999) Electrostatic zipper motif for DNA aggregation. *Phys. Rev. Lett.* **82**, 4138–4141
51. Todd, B. A., Parsegian, V. A., Shirahata, A., Thomas, T. J., and Rau, D. C. (2008) Attractive forces between cation condensed DNA double helices. *Biophys. J.* **94**, 4775–4782
52. Woldringh, C. L., Jensen, P. R., and Westerhoff, H. V. (1995) Structure and partitioning of bacterial DNA: determined by a balance of compaction and expansion forces? *FEMS Microbiol. Lett.* **131**, 235–242
53. Zimmerman, S. B., and Murphy, L. D. (1996) Macromolecular crowding and the mandatory condensation of DNA in bacteria. *FEBS Lett.* **390**, 245–248
54. Norris, V. (1995) Hypothesis: chromosome separation in *Escherichia coli* involves autocatalytic gene expression, transertion and membrane-domain formation. *Mol. Microbiol.* **16**, 1051–1057
55. Libby, E. A., Roggiani, M., and Goulian, M. (2012) Membrane protein expression triggers chromosomal locus repositioning in bacteria. *Proc. Natl. Acad. Sci. U.S.A.* **109**, 7445–7450
56. Rudolph, C. J., Upton, A. L., and Lloyd, R. G. (2007) Replication fork stalling and cell cycle arrest in UV-irradiated *Escherichia coli*. *Genes Dev.* **21**, 668–681
57. Minsky, A., Shimoni, E., and Frenkiel-Krispin, D. (2002) Stress, order and survival. *Nat. Rev. Mol. Cell Biol.* **3**, 50–60
58. Minsky, A. (2003) Structural aspects of DNA repair: the role of restricted diffusion. *Mol. Microbiol.* **50**, 367–376
59. Kornyshev, A. A., and Leikin, S. (2001) Sequence recognition in the pairing of DNA duplexes. *Phys. Rev. Lett.* **86**, 3666–3669
60. Kornyshev, A. A., and Wynveen, A. (2009) The homology recognition well as an innate property of DNA structure. *Proc. Natl. Acad. Sci. U.S.A.* **106**, 4683–4688
61. Inoue, S., Sugiyama, S., Travers, A. A., and Ohyama, T. (2007) Self-assembly of double-stranded DNA molecules at nanomolar concentrations. *Biochemistry* **46**, 164–171
62. Wang, X., Zhang, X., Mao, C., and Seeman, N. C. (2010) Double-stranded DNA homology produces a physical signature. *Proc. Natl. Acad. Sci. U.S.A.* **107**, 12547–12552
63. Cherstvy, A. G. (2011) DNA-DNA sequence homology recognition: physical mechanisms and open questions. *J. Mol. Recognit.* **24**, 283–287
64. Ström, L., Lindroos, H. B., Shirahige, K., and Sjögren, C. (2004) Postreplicative recruitment of cohesin to double strand breaks is required for DNA repair. *Mol. Cell* **16**, 1003–1015
65. Cox, M. M. (1998) A broadening view of recombinational DNA repair in bacteria. *Genes Cells* **3**, 65–78
66. Cox, M. M., Goodman, M. F., Kreuzer, K. N., Sherratt, D. J., Sandler, S. J., and Mariani, K. J. (2000) The importance of repairing stalled replication forks. *Nature* **404**, 37–41
67. Michel, B., Flores, M. J., Viguera, E., Grompone, G., Seigneur, M., and Bidnenko, V. (2001) Rescue of arrested replication forks by homologous recombination. *Proc. Natl. Acad. Sci. U.S.A.* **98**, 8181–8188
68. Kuzminov, A. (2001) DNA replication meets genetic exchange: Chromosomal damage and its repair by homologous recombination. *Proc. Natl. Acad. Sci. U.S.A.* **98**, 8461–8468
69. Cox, M. M. (2002) The nonmutagenic repair of broken replication forks via recombination. *Mutat. Res.* **510**, 107–120
70. Lusetti, S. L., and Cox, M. M. (2002) The bacterial RecA protein and the recombinational DNA repair of stalled replication forks. *Annu. Rev. Biochem.* **71**, 71–100
71. McGlynn, P. (2004) Links between DNA replication and recombination in prokaryotes. *Curr. Opin. Gen. Dev.* **14**, 107–112
72. Goobes, R., and Minsky, A. (2001) Thermodynamic aspects of triplex DNA formation in crowded environments. *J. Am. Chem. Soc.* **123**, 12692–12693
73. Levin-Zaidman, S., Englander, J., Shimoni, E., Sharma, A. K., Minton, K. W., and Minsky, A. (2003) Ringlike structure of the *Deinococcus radiodurans* genome: A key to radioresistance? *Science* **299**, 254–256